JACC: BASIC TO TRANSLATIONAL SCIENCE VOL. 6, NO. 5, 2021

PRECLINICAL RESEARCH

Can a Biohybrid Patch Salvage Ventricular Function at a Late Time Point in the Post-Infarction Remodeling Process?

Lindemberg M. Silveira-Filho, MD, PhD,[a,b] Garrett N. Coyan, MD, MS,[a,c] Arianna Adamo, MS,[a] Samuel K. Luketich, MS,[a] Giorgio Menallo, BSc, MSc,[a,c] Antonio D'Amore, PhD,[a,c,d] William R. Wagner, PhD[a,c]

VISUAL ABSTRACT

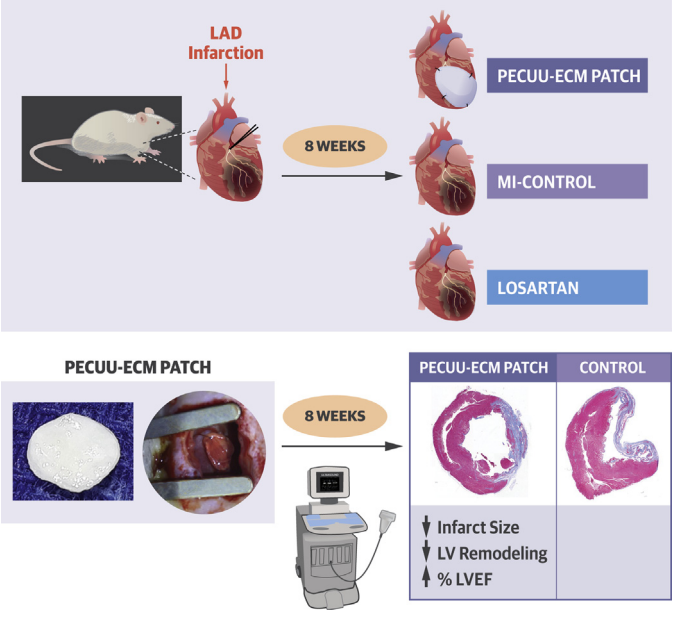

Silveira-Filho, L.M. et al. J Am Coll Cardiol Basic Trans Science. 2021;6(5):447–63.

HIGHLIGHTS

- A simple, biohybrid patch made of polymer (PECUU) and ECM, without cellular components, was able to induce positive remodeling features when applied over chronic infarcts with severely dilated hearts and high cardiac function impairment in rats.
- The remodeling benefit was particularly notable in a subgroup of the sickest rats with very low initial ejection fraction in which the echocardiographic endpoints were found to improve after treatment.
- This technological approach may hold promise for future translation to patients in a chronic scenario.

From the [a]McGowan Institute for Regenerative Medicine, University of Pittsburgh, Pittsburgh, Pennsylvania, USA; [b]Department of Surgery, University of Campinas, Sao Paulo, Brazil; [c]Department of Bioengineering, Department of Surgery, University of Pittsburgh, Pittsburgh, Pennsylvania, USA; and [d]RiMED Foundation, Palermo, Italy.

The authors attest they are in compliance with human studies committees and animal welfare regulations of the authors' institutions and Food and Drug Administration guidelines, including patient consent where appropriate. For more information, visit the Author Center.

Manuscript received October 19, 2020; revised manuscript received January 7, 2021, accepted January 7, 2021.

ISSN 2452-302X https://doi.org/10.1016/j.jacbts.2021.01.004

JACC: BASIC TO TRANSLATIONAL SCIENCE VOL. 6, NO. 5, 2021
MAY 2021:447–63

ABBREVIATIONS AND ACRONYMS

AT_1R = angiotensin 1 receptor
ECM = extracellular matrix
EDA = end-diastolic area
EF = ejection fraction
ESA = end-systolic area
FS = fractional shortening
HF = heart failure
LV = left ventricle
LVdd = left ventricular end-diastolic diameter
LVEF = left ventricular ejection fraction
LVFW = left ventricular free wall
LVsd = left ventricular end-systolic diameter
M1 = macrophage type 1
M2 = macrophage type 2
MI = myocardial infarction
MT = Masson trichrome
PBS = phosphate-buffered saline
PECUU = poly(ester carbonate urethane) urea
PEUU = poly(ester urethane) urea
SMA = smooth muscle actin

SUMMARY

A biohybrid patch without cellular components was implanted over large infarcted areas in severely dilated hearts. Nonpatched animals were assigned to control or losartan therapy. Patch-implanted animals responded with better morphological and functional echocardiographic endpoints, which were more evident in a subgroup of animals with very low pre-treatment ejection fraction (<35%). Patched animals also had smaller infarcts than both nonpatched groups. This simple approach could hold promise for clinical translation and be applied using minimally invasive procedures over the epicardium in a large set of patients to induce better ventricular remodeling, especially among those who are especially frail. (J Am Coll Cardiol Basic Trans Science 2021;6:447–63)

Over the past 2 decades, patch placement onto the epicardial wall following myocardial infarction (MI) has been a widely investigated therapy in a large preclinical trial and several clinical trials, aiming to preserve or improve ventricular function and change the course of post-MI ventricular remodeling (1-3). Although many of these patches have sought to deliver cellular or pharmaceutical elements, the notion that simply applying a biodegradable, without cellular components, temporary mechanical support to the infarcted wall has shown merit, at least in preclinical models (4). In 2016, D'Amore et al. (5) showed that a bilayered poly(ester carbonate urethane) urea (PECUU)-extracellular matrix (ECM) biohybrid patch improves echocardiographic cardiac function and angiogenesis in rats when implanted 2 weeks post-MI. That study demonstrated the value of combining ECM digest components with a biodegradable elastomer to form a biohybrid material. The synthetic elastic component used was similar to materials that had been shown in previous studies to provide functional benefit as a patch material in rat and porcine models (3,5-7).

The role of timing of post-MI application of biomaterial patches and the level of functional recovery that might be achieved have not been well addressed. Most reported patch implant studies were performed in the first several days after infarct induction (4,6). However, despite widespread use of early percutaneous revascularization after acute MI, many patients, when referred for treatment, have already experienced extensive ventricular thinning, scarring, and functional deterioration and developed dilated cardiomyopathy and progressive heart failure (HF). At this stage, a strict drug regimen may be required to maintain function and decrease mortality (8).

An important question for the translation of cardiac patch approaches to the clinic is whether patch application at later time points, after extensive remodeling and loss of function have occurred, would still provide benefit. This study specifically aimed to examine whether a biohybrid PECUU-ECM patch applied over a chronic left ventricular (LV) infarct in a rat model could provide functional benefit after much of the adverse ventricular remodeling had already occurred, and how this therapy compares to angiotensin 1 receptor (AT_1R) blocker treatment.

METHODS

PATCH FABRICATION. Cardiac patches were fabricated by a modified 2-stream electrospinning process to combine PECUU with ECM (5). The biodegradable elastic polymer PECUU was synthetized as previously described (9). Briefly, ECM was obtained from porcine hearts (Thoma Meat Market, Saxonburg, Pennsylvania) and decellularized according to a standard protocol (5,9). Particulate ECM was enzymatically digested at a concentration of 20 mg/ml ECM per milliliter using 2 mg/ml pepsin (Sigma-Aldrich, St. Louis, Missouri) in 0.01 M HCl for 48 h at room temperature. Digested ECM was neutralized on ice with 1:10 of the digest volume of 0.1 M NaOH and 1:9 of the digest volume of 10× phosphate-buffered saline (PBS), and further diluted to a final ECM concentration of 15 mg/ml using 1× PBS (5). PECUU was dissolved in hexafluoroisopropanol (12% weight/volume). For the material used to make the patch, 2 distinct layers were created by sequential 20-min deposition periods. Fiber deposition was concentrated on a well-defined conductive area of a rotating steel cylinder (diameter 1/4; 114 mm) (**Figure 1A**). Two concurrent depositing streams (one with PECUU solution emitted at 20 ml/h from a 10-cm distance and 13-kV charge, and a second with PBS at 1.35 ml/min

from 4-cm distance and 8-kV charge) were used to first deposit the polymer-rich layer. For the ECM-rich layer, identical parameters were utilized for the PECUU stream, while the second stream was switched to ECM solution emitted at 1.35 ml/min from a 4-cm distance and at a 13-kV charge. After the deposition period, the scaffold material was cut from the cylinder and incubated at 37°C for 45 min to induce ECM solution gelation. The process resulted in a patch comprising 2 layers, with 1 side enriched in PECUU and the other side with ECM deposited between PECUU fibers. The patches used for placement over infarcts were cut into 6-mm disks using a surgical punch (**Figure 1B**) and sterilized by ultraviolet light before implantation. Patch samples were also utilized for pre-implant biaxial mechanical testing (Supplemental Figure 1).

ANIMAL PROTOCOL. Adult female Lewis rats (weight ≅200 g) (Harlan Sprague Dawley, Indianapolis, Indiana) were used following animal care and surgical protocols in accordance with the National Institutes of Health Guidelines for Animal Care and a protocol approval by the University of Pittsburgh Institutional Animal Care and Use Committee. Infarction was induced by a left anterior descending artery ligation protocol (4,5). Briefly, rats were anesthetized with isoflurane (5.0% induction and 1.25% to 1.5% maintenance with 100% oxygen), intubated, and mechanically ventilated with a rodent 683 ventilator (Harvard Apparatus, Holliston, Massachusetts). Tidal volume was set to 0.6 to 2 ml of body weight and respiratory frequency 70/min. Animals were placed on a warming pad (37°C) in the supine position, and the anterior chest was trimmed. Lidocaine (10 mg/kg) and cefazolin (100 mg/kg) were administered intramuscularly for arrhythmia and infection prophylaxis. Left chest skin was sterilized with povidone-iodine solution. Animals underwent left thoracotomy at the fourth intercostal space. The left anterior descending artery was identified and ligated with a 6.0 polypropylene suture below the edge of left atrial appendage. The infarct could be identified visually by color change in the subjacent segment. Lungs were reinflated bilaterally to prevent pneumothorax after chest closure. Layers were closed with 4.0 polyglactin suture (Vicryl, Ethicon Inc., Somerville, New Jersey) and the animals allowed to recover. Intramuscular buprenorphine (0.05 mg/kg) was administered to all animals for 3 days after surgery.

After 5 days, the animals underwent echocardiography to evaluate the percentage of induced akinetic or dyskinetic regions to left ventricular free wall (LVFW) area (5). Animals with infarcts of at least 25% of the LVFW remained on the protocol. Those that did not develop adequate infarct size were euthanized. Animals in the protocol (n = 49) were then randomized to 1 of 3 groups: 1) group P: MI + PECUU-ECM patch; 2) group C: MI control (MI and no patch implantation); or 3) group L: MI control (MI and no patch implantation) + oral intake of losartan 15 mg/kg.

Immediately after echocardiographic confirmation of infarcts, the animals in group L started receiving daily oral losartan, diluted in water and sucrose. Losartan administration to this group was continued throughout the protocol. After 8 weeks, the animals were anesthetized similarly to the MI induction surgery. All underwent echocardiographic assessment as baseline pre-treatment (8 weeks post-MI) and then a second left thoracotomy at the fourth intercostal space. Each heart was exposed and the infarcted anterior wall segment identified by its pale white color and abnormal contractility. In animals previously randomized to the patch implant (group P), the epicardial infarcted segment was lightly abraded and the patch sutured to the wall over the infarct area with continuous 6.0 polypropylene (**Figure 1C**). The patch surface that was enriched in ECM was always placed down on the infarct so that is was in contact with the epicardium, and the PECUU surface was face up. Animals in the control (C) and losartan (L) groups had a sham surgical procedure wherein the infarcted segment was lightly abraded but no patch was implanted. All surgical wounds were closed and the animals allowed to recover.

Animals were euthanized 8 weeks after the treatment surgery (16 weeks post-MI induction) and the hearts harvested (**Figure 1D**). Healthy controls of similar weight and age that were not subject to MI or other surgery were followed as the healthy control group.

ECHOCARDIOGRAPHY. All animals underwent echocardiographic assessment at baseline (pre-treatment, immediately before treatment surgery, which corresponded to 8 weeks after MI) and at 2, 4, and 8 weeks post-treatment, when they were euthanized (8 weeks post-treatment surgery and 16 weeks post-MI induction). Rats were anesthetized with 1.5% isoflurane and 100% oxygen inhalation. Standard echocardiography was performed using an Acuson Sequoia C256 system with a 13-MHz linear ultrasonic transducer (15L8, Acuson Corporation, Mountain View, California) in a phased-array format. Two-dimensional cross-sectional measurements in the LV short-axis view at the papillary muscle level were recorded. End-diastolic (EDA) and end-systolic (ESA) LV internal cavity areas were measured by tracing the endocardial border. LV end-diastolic diameter (LVdd) and LV end-systolic diameter (LVsd) were traced

FIGURE 1 PECUU-ECM Patch Fabrication: Pre-Implant and Surgical Views

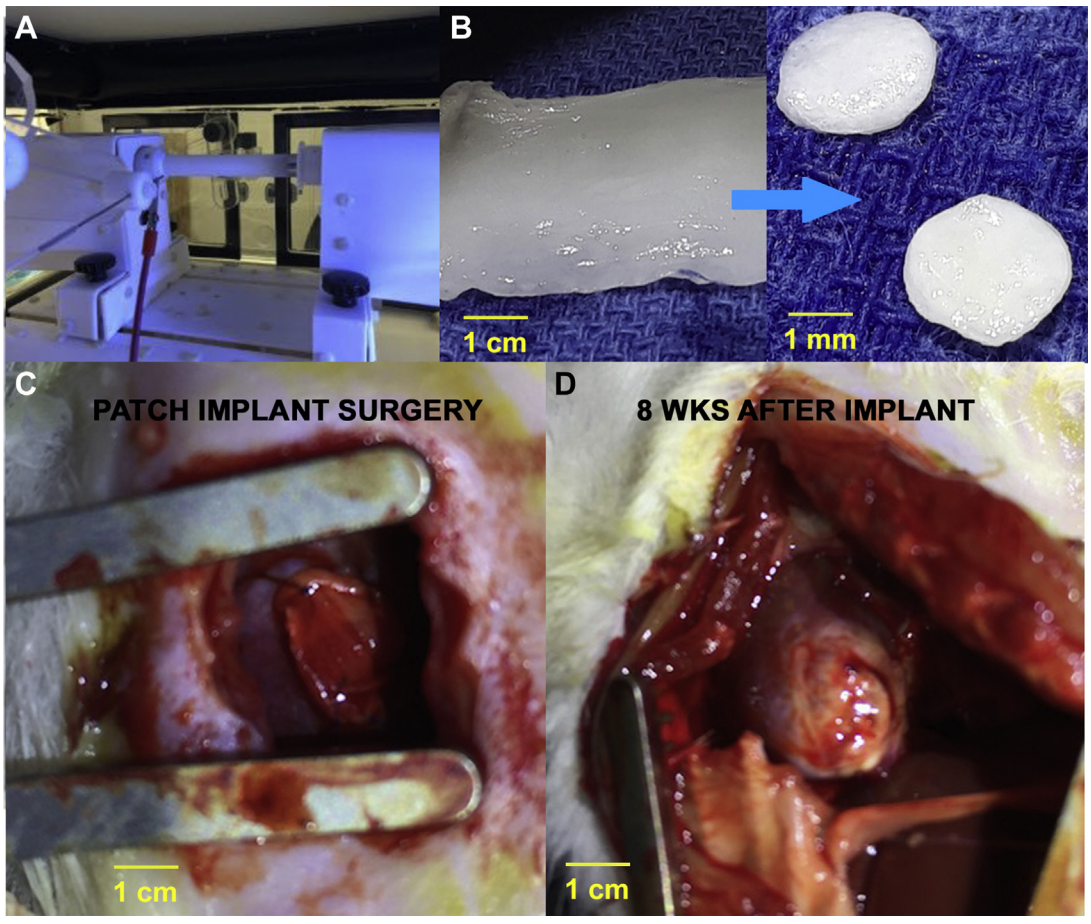

(A) Electrospinning device. Polymer and ECM are deposited over the rotating mandrel. **(B)** The bilayered PECUU-ECM patch is removed from the electrospinning device and sliced into 6-mm-diameter patch disks. The upper surface is the ECM-rich side that will be placed in contact with the epicardium. **(C)** Patch surgically applied over the left ventricular (LV) infarcted segment, 8 weeks post-myocardial infarction (MI). **(D)** Patch-implanted heart 16 weeks post-MI (after euthanasia) showing the scaffold integrated with the LV wall. ECM = extracellular matrix; PECUU = poly(ester carbonate urethane) urea; wks = weeks.

longitudinally over the acquired images with M-mode confirmation. LV end-diastolic volume (LVdv), LV end-systolic volume (LVsv), percent fractional area change (%FAC), percent fractional shortening (%FS), and left ventricular ejection fraction (LVEF) were calculated as follows (5):

$$\%FAC = [EDA - ESA/EDA] \times 100\%$$

$$LVdv = (7.0/(2.4 + LVdd) \times 3LVdd)$$

$$LVsv = (7.0/(2.4 + LVsd) \times 3LVsd)$$

$$\%FS = LVdd - LVsd/(LVdd \times 100)$$

$$LVEF = LVdv - LVsv/(LVdv \times 100)$$

All measurements were performed using the OsiriX digital image processing application, version 3.7.1 (Pixmeo, Co., Geneva, Switzerland). The timeline of the study protocol is shown in Figure 2.

HISTOLOGY. Whole-heart explants were fixed in 2% paraformaldehyde for 7 days, sectioned at 10-μm thickness in the LV transverse direction, mounted on glass slides, and stained with Masson trichrome (MT) and hematoxylin-eosin. Cellular infiltration and its relation to the infarcted region, infarct transition zone, and patch material were evaluated.

QUANTIFICATION OF MUSCLE, SCAR AREA, AND LV ANTERIOR WALL THICKNESS. LV cross-sections stained with MT were utilized to quantify muscle, scaffold/newly formed tissue, scar area, and wall thickness (5,9). Scar and muscle areas were measured on ImageJ software using (National Institutes

of Health, Bethesda, Maryland) computer-based planimetry. A digital frame of constant size was applied to each sample to extract scar area, muscle areas, and total LV area in the explanted hearts in order to eliminate the variability induced by different heart sizes or differences in sectioning plane. Scar, scaffold/new tissue, and muscle indices were defined as the ratio between the scar or muscle area and the total area occupied by the explants. LV anterior wall thickness was calculated as: LV thickness = scar area/[(epicardial circumference + endocardial circumference) / 2] (5,10).

IMMUNOFLUORESCENCE. Sample hearts were fixed in 4% paraformaldehyde solution for 4 h, immersed in sucrose solution overnight, embedded with OCT compound (Tissue-Tek, Torrance, California), and sectioned in 10-μm step sizes using a microtome. For immunohistochemical staining, tissue sections were incubated for 20 min at 70°C in antigen retrieval Histo VT One (Nacalai Tesque, Kyoto, Japan) diluted 10× in deionized water, then blocked for 3 h with 2% bovine serum albumin and 10% goat serum in 0.2% Triton-PBS solution at room temperature. For blood vessel identification, sections were incubated with mouse primary antibody against CD31 1:100 (Ab64543, Abcam, Cambridge, United Kingdom) and rabbit primary antibody against alpha-smooth muscle actin (SMA) 1:200 (Ab5694, Abcam). Antirabbit Alexa Fluor 594 1:1000 (A21207, Invitrogen), biotinylated anti-mouse 1:200 (BA-2001, Vector Laboratories, Burlingame, California), and Streptavidin-Alexa Fluor 488 conjugate 1:150 (S32354, Invitrogen, Waltham, Massachusetts) were utilized as secondary antibodies; and 4′,6-diamidino-2-phenylindole (DAPI H-1200, Vectashield, Vector Laboratories) was utilized for nuclear staining. Multispectral epifluorescent images were acquired using a Nikon Eclipse 6600 microscope (Nikon Corporation, Tokyo, Japan), with spectral unmixing to remove autofluorescence performed using Nuance 3.0.2 software (Caliper Life Science Inc., Hopkinton, Massachusetts). For each slide, 10 fields were acquired at 200× in proximity to suture areas, around the implanted patch, and at the intersection with the infarcted region. In the nonpatched animals, images were obtained in similar topography, over the infarcted area and its border zone. CD68- and CD163-positive cells were identified with custom-made software developed in MATLAB (MathWorks, Natick, Massachusetts) (10).

Cell number was obtained by the ratio between mean cell pixel size and total number of marker positive pixels, which also enabled calculation of the CD163/CD68 ratio. A similar image segmentation process enabled identification of α-SMA-positive pixels and cell nuclear aspect ratio, defined as the ratio between the major and minor nuclei axes (5,9). A total of 5 independent samples from each group was used for immunofluorescence analysis. Images were acquired from the transition zone between the infarct border and healthy tissue and scarred tissue. In the patched animals, images were obtained in the scarred tissue and its close relation to the PECUU-ECM patch.

FIGURE 2 Timeline of Study Protocol

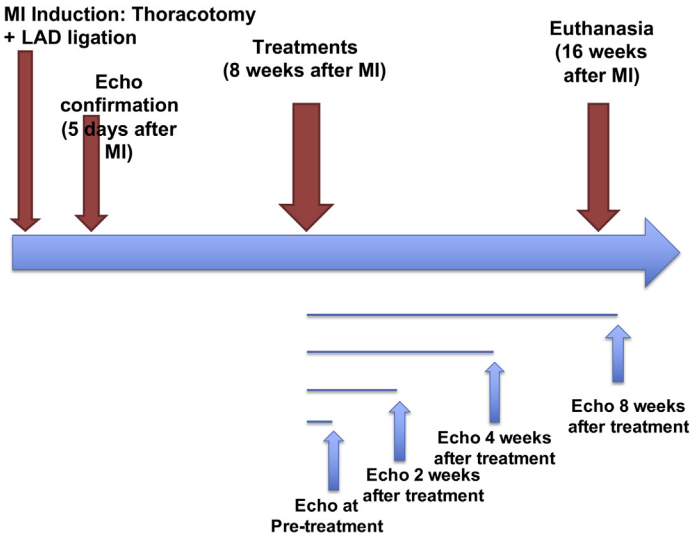

Randomization was performed 5 days after induction of myocardial induction (MI), when the animals in the losartan group started receiving the drug orally.
Echo = echocardiography; LAD = left anterior descending artery.

MECHANICAL COMPLIANCE TESTS. Ex vivo mechanical global compliance tests were performed to evaluate LV global mechanics. Explanted hearts were tested within 6 h of animal death. A collapsed size 5 latex balloon mounted on a flexible catheter (AD Instruments, Dunedin, New Zealand) was introduced into the explanted LV through the aorta. The tests were conducted under quasistatic conditions (0.25 ml/min) in pressure-control mode, after 5 cycles of preconditioning, reaching a peak pressure of 200 mm Hg to ensure proper contact between the endocardium and the balloon. The catheter was equipped with a Mikro-Cath (Millar Inc., Houston Texas) and fed by water using a Ph2000 pump (Harvard Bioscience, Holliston, Massachusetts). Pressure and volume signals were acquired using an NISBC68 (National Instruments, Austin, Texas) and a custom-made script developed in LabVIEW 13.0

TABLE 1 Incidence of Death in Animals During Interval Between Treatment Application (8 Weeks After MI) and Euthanasia (16 Weeks After MI)

	Number of Animals	Deaths
Patch	21	1 (4.75)
MI control	18	5 (27.7)
Losartan	10	0 (0.0)
		p = 0.064

Values are n or n (%). A total of 49 animals randomized to a treatment group and 8 healthy controls were followed. Forty-three rats finished the protocols. There was a higher tendency for death in the myocardial infarction (MI) control group compared to the losartan or patch groups, although this did not reach statistical significance (p = 0.064).

(National Instruments) as previously described (5). The pump was able to impose LV volume variations, and the same catheter was used to obtain the pressure measurements.

STATISTICAL ANALYSIS. Statistical analysis was performed using GraphPad Prism (GraphPad Software, San Diego, California). Normal distribution was verified by the D'Agostino-Pearson normality test. Analysis of variance followed by Tukey multiple comparison test was utilized for comparison of multiple samples. Changes over time, when appropriate, were evaluated with the paired Student's *t*-test. When the data were not normally distributed, the Kruskal-Wallis nonparametric multiple comparison test was used. The Fisher exact test was applied to compare death rates among animals. Results are presented as mean ± SEM, and differences were considered to be statistically significant at $p < 0.05$.

RESULTS

MATERIAL CHARACTERIZATION. The bilayered patch structure was verified visually, morphologically, and physically by handling the specimens. Structural continuity between the 2 layers with no delamination was confirmed. Patch tensile mechanical response, as characterized by biaxial testing, was compared to LV samples from rat hearts. The PECUU-ECM patch exhibited an isotropic response, similar in behavior and modulus to polymer patches in earlier studies (3,9) (Supplemental Figure 1), and was distinct from the anisotropic behavior of freshly isolated healthy rat LV wall samples.

ECHOCARDIOGRAPHY. Forty-nine animals with MI area >25% of LVFW participated in the protocol. A total of 43 animals completed the 8-week post-treatment protocol. Overall, more animals died after treatment in the MI control group (sham surgery) than in either the losartan or patch group, although there were no significant differences (p = 0.064) (Table 1). All investigated groups showed deteriorated echocardiographic functional endpoints compared to healthy controls (Figure 3). Representative echocardiographic images are shown in Figure 4 and Video 1. Nonpatched groups showed more evident dilation, whereas patch-implanted animals 8 weeks post-treatment show less spheric LV geometry compared to both nonpatched groups and were more similar to healthy controls. Contractility indices %FS and LVEF were higher in animals in the patch-treated group than in the control and losartan groups at 4 and 8 weeks after treatment. No differences were found between losartan and control animals (Figures 5A and 5B). EDA, ESA (Figures 5C and 5D), and both LV diameters increased from post-infarct pre-treatment to 8 weeks post-treatment in the 2 nonpatched groups (control and losartan). No differences according to time were found in the patch group.

In a subgroup of 27 animals with very low post-infarct ejection fraction (EF) (<35%) pre-treatment, EF and %FS were higher at 4 and 8 weeks after treatment in the patched animals than in nonpatched animals. Furthermore, LVEF and %FS increased intragroup in patched animals from pre-treatment to 8 weeks post-treatment, which was not seen in the control and losartan groups (Figure 6).

HISTOLOGY. All isolated LVs showed transmural infarcts and the PECUU-ECM patch applied over infarcted tissue. In sections stained with hematoxylin-eosin, the patched region of the infarcted wall had substantial cellular infiltration. The losartan and control groups both presented with scarred walls and lower cellular content. In MT-stained sections, the patches were implanted over the infarcted segment, with tissue thickness maintenance and cell infiltration around the patch close to infarcted area, whereas samples from both nonpatched hearts groups showed larger scarred areas that were narrow in width (Figure 7). Macroscopically, patches were integrated into infarcted tissue and were not fully degraded. As large infarcts developed, the patches could not cover the whole dyskinetic area (Figures 8A and 8B). Nonpatched hearts developed wide dyskinetic areas with very thin scarred tissue (Figures 8C and 8D).

SCAR AREA, MUSCLE TISSUE THICKNESS, PERCENT INFARCT SIZE, AND IMMUNOFLUORESCENCE. Scar area did not show differences according to treatment, as all enrolled animals developed large transmural infarcts during the extended period after infarct induction but before intervention (Supplemental Figure 2). The percent infarct size related to healthy tissue was lower in patch-treated animals than in

FIGURE 3 Echocardiographic Assessment of All Groups Compared to Healthy Controls

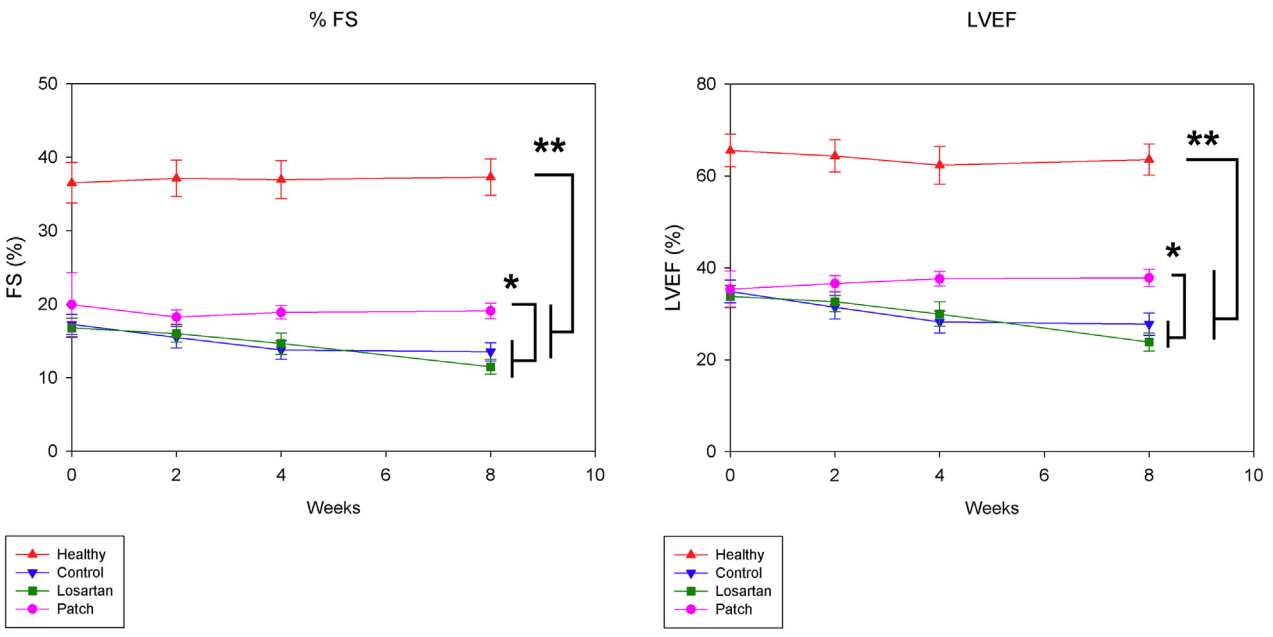

Percent fractional shortening (FS) and left ventricular ejection fraction (LVEF) in all groups were significantly lower than in healthy animals, but both endpoints were better in patch animals than in animals in the control and losartan groups at 4 and 8 weeks post-treatment. Data are expressed as mean ± SEM. *$p < 0.05$; **$p < 0.001$.

both control and losartan animals (Figure 9A). LV thickness was higher in the patched animals, but the difference was not significant ($p = 0.055$) (Figure 9B). When assessing the subgroup of rats with initial pre-treatment EF <35%, percent infarct size was lower in patched animals (Figure 9C), and LV thickness showed no difference (Figure 9D). Staining with 4′,6-diamidino-2-phenylindole to identify overall cell nuclei did not show differences among groups. Macrophage marker CD68 staining was higher in the animals receiving losartan throughout the study. $CD163^{+}/CD68^{+}$ ratio and αSM^{A+} cells did not differ among groups (Supplemental Figure 3).

MECHANICAL COMPLIANCE. In global compliance tests with LV pressure-volume relationship measurements, both groups of infarcted animals (patch-treated and control) showed much greater compliance than the healthy control hearts. However, the patched ventricles exhibited stiffer passive behavior than the controls (Figure 10).

DISCUSSION

In this study, a biohybrid patch made from a degradable elastomer (PECUU) and ECM-based hydrogel was implanted over the infarcted segment in a rat model 8 weeks after MI induction. Patches were surgically implanted over large infarcted areas in severely dilated hearts. Nonpatched animals were assigned to an MI control group or a group that started receiving the AT_1R blocker losartan 5 days after MI. Patch-implanted animals evolved overall with better morphological and functional echocardiographic endpoints 8 weeks post-treatment (16 weeks in total after MI) versus both nonpatched groups. EF and %FS improved in patched animals from pre-treatment to 4 and 8 weeks post-treatment, which was more evident when a subgroup of very low EF (<35%, pre-treatment) animals was studied. Losartan was not related to echocardiographic improvement compared to controls, but fewer animals in the losartan group than in control group died during the protocol. Patched animals also presented smaller infarcts compared to both nonpatched groups, and passive global compliance tests showed stiffening of the LV in association with patch treatment.

PECUU-ECM PATCH. The biohybrid PECUU-ECM patch used in this study combines advantages from a biodegradable polymer scaffold, such as higher anisotropy and mechanical support, and putative

FIGURE 4 Echocardiographic Images of Two-Dimensional, Cross-Sectional, Parasternal Short Axis

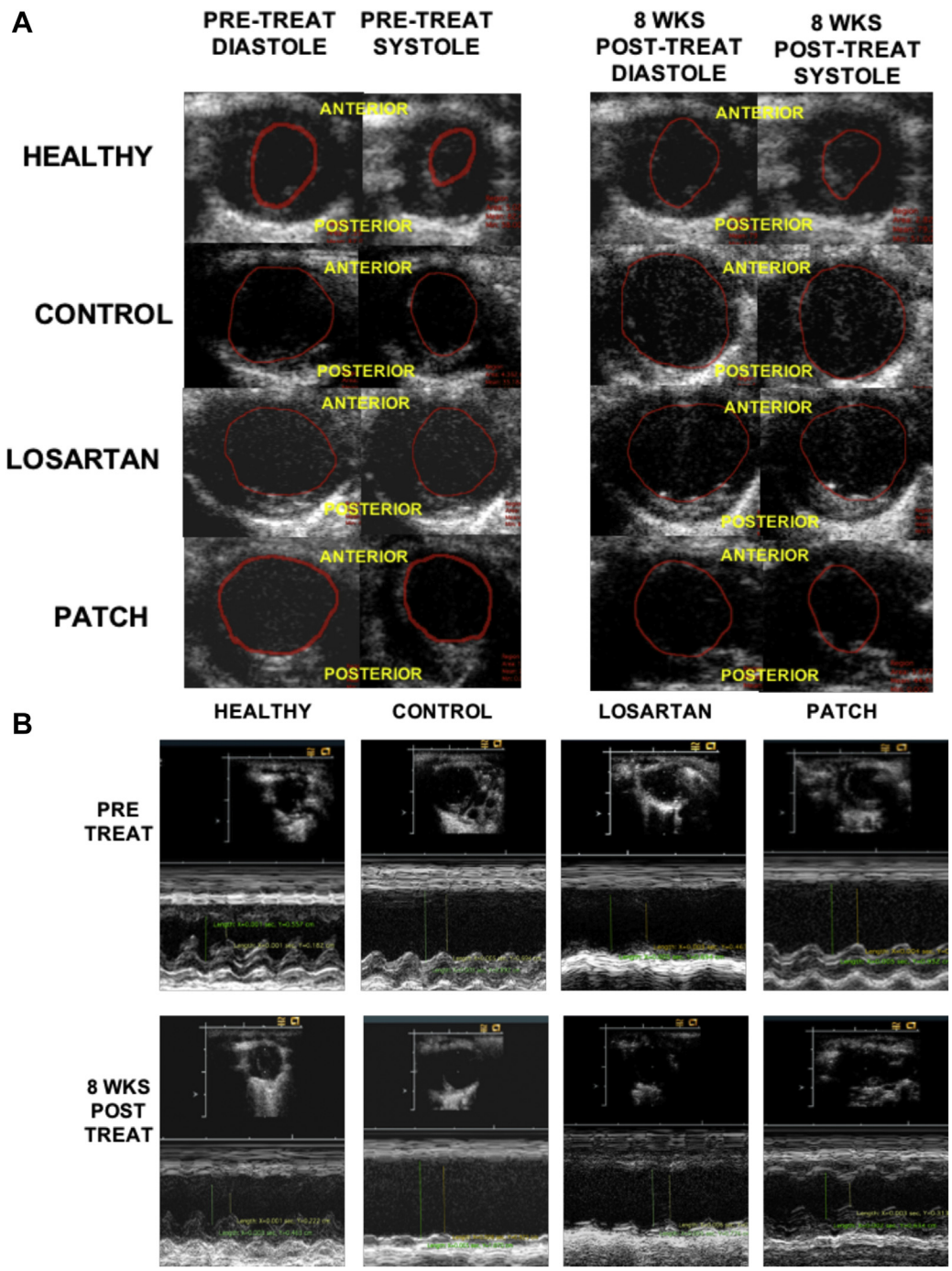

Images in diastole and systole at pre-treatment (8 weeks post-MI) and 8 weeks post-treatment (16 weeks post-MI) time points. **(A)** Endocardial borders are highlighted in both diastole and systole. **(B)** All infarcted hearts pre-treatment show worse systolic function compared to hearts from the healthy group. At 8 weeks post-treatment, both control MI and losartan groups developed severe dilation and higher sphericity, whereas patched animals exhibited less dilation and an LV geometry closer to that of healthy animals. MI = myocardial infarction; wks = weeks.

FIGURE 5 Echocardiographic Assessment of All 43 Infarcted Animals

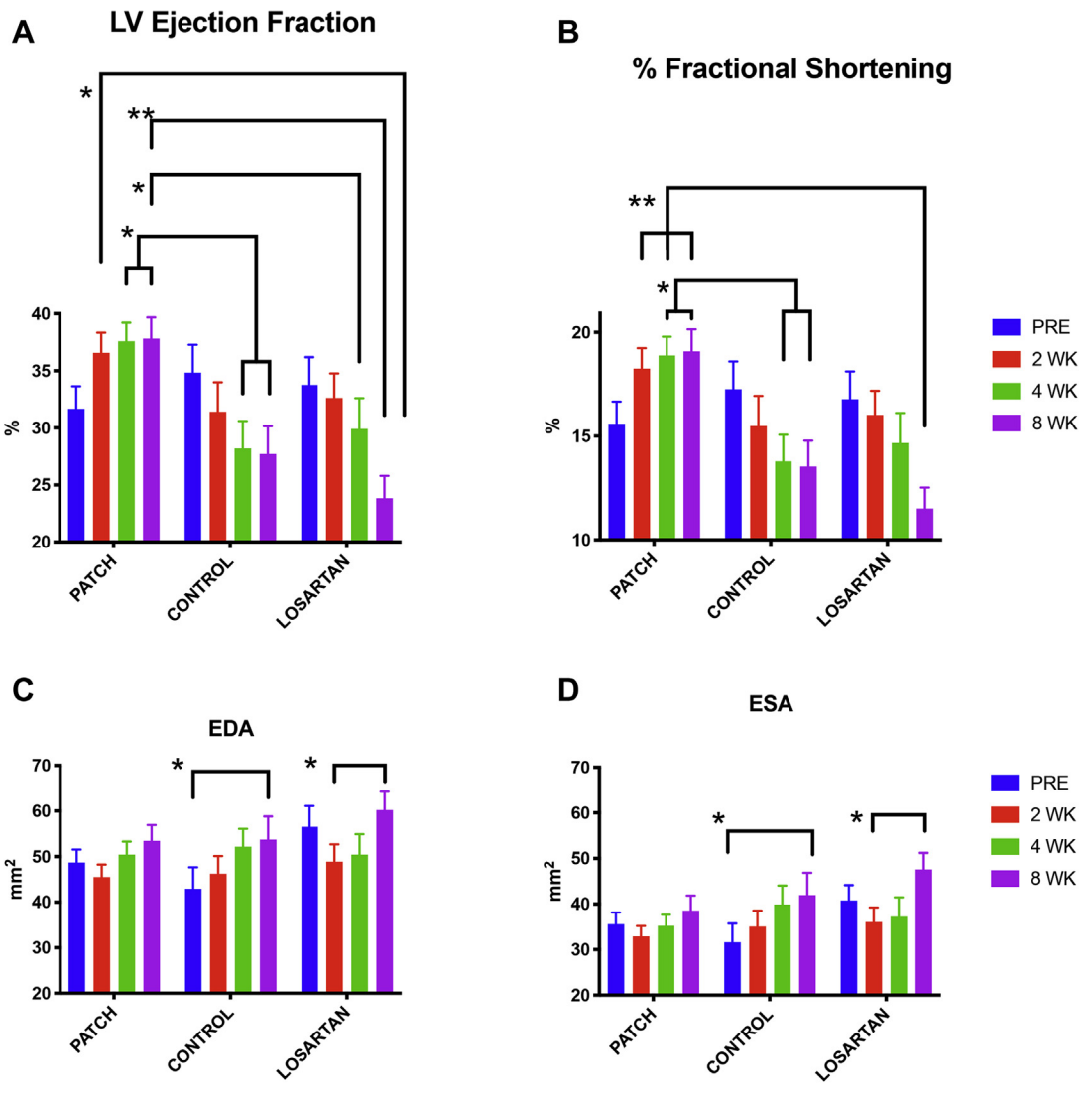

Data for pre-treatment and 2, 4, and 8 weeks post-treatment. **(A)** Left ventricular (LV) ejection fraction 4 and 8 weeks after treatment was higher in the patch group than in both the losartan and control groups at the same time period. At 2 weeks after treatment, LV ejection fraction was higher in the patch group than in the losartan group at 8 weeks post-treatment. **(B)** Percent fractional shortening was higher at 2, 4, and 8 weeks after treatment in the patch group than in the losartan group 8 weeks after treatment. Percent fractional shortening in the patch group at 4 and 8 weeks after treatment was higher than in the control group at 4 and 8 weeks after treatment. **(C, D)** LV end-diastolic area (EDA) and end-systolic area (ESA) increased in the control and losartan groups from pre-treatment to 8 weeks post-treatment, whereas no difference was verified in the patch group. Data are expressed as mean ± SEM. *$p < 0.05$; **$p < 0.01$. wks = weeks.

ECM-derived bioactive features. ECM (or, more specifically in this case, gel derived from decellularized tissue) has been demonstrated to be a reservoir of bioactive growth factors and matricellular proteins that enable bioinductive effects (11). Mewhort et al. (12) verified in a rat infarct model that when intact and chemically inactivated ECM patches were compared, both induced the same LV thickness. However, intact ECM patches were related to a provasculogenic paracrine response, lower LV dilation, and progressive improvement in LVEF compared to inactivated patches. Biodegradable polymer patches, such as poly(ester urethane) urea (PEUU), have been related to induction of α-SMA cells beneath the implanted patches, possibly inducing bioactivation of progenitor contractile smooth muscle cells (3). For

FIGURE 6 Echocardiographic Assessment of Animals With Pre-Treatment LVEF <35% (8 Weeks After MI Induction, at Pre-Treatment)

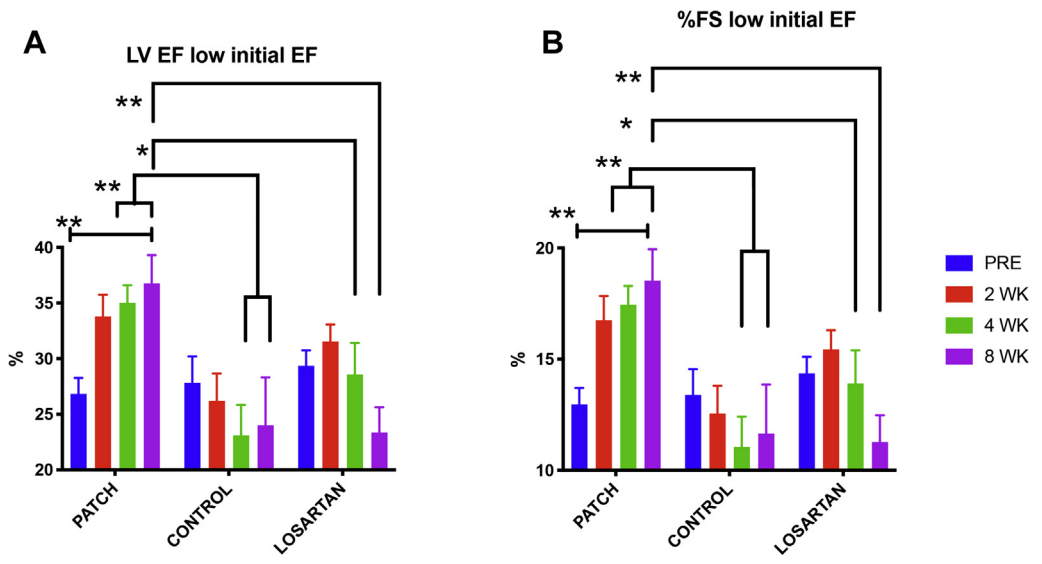

Data for pre-treatment and 2, 4, and 8 weeks post-treatment for the subgroup of 27 animals. Both EF **(A)** and %FS **(B)** improved in patch-treated animals from pre-treatment to 8 weeks post-treatment ($p < 0.01$). This was not seen in the control or losartan groups. Patch-treated animals presented higher EF and %FS at 4 and 8 weeks post-treatment than both control and losartan groups at the same time period. Data expressed as mean ± SEM. *$p < 0.05$; **$p < 0.01$. Abbreviations as in Figures 3 and 5.

example, as PEUU degrades, macrophages and fibroblasts infiltrate the implanted area.

PECUU is a polymer with partial substitution of polyester segments with polycarbonate, which results in slower degradation behavior (13). When PECUU was compared to PEUU (which has a faster degradation rate) as a patch applied over infarcted hearts, PECUU showed greater vascular density and better LV contractility after 16 weeks and a greater macrophage type 2 (M2) to macrophage type 1 (M1) phenotype in the infarct region. These results emphasize the importance of specific polymer selection and the potential effect of degradation rates.

D'Amore et al (5) implanted this PECUU-ECM patch and compared it to electrospun PECUU without ECM. The biohybrid combination was related to higher vascular infiltration and better M2 expression (5). The PECUU-ECM patch also was able to mechanically reduce compliance and enhance LV chamber stiffening in the treated hearts. Therefore, the biohybrid PECUU-ECM patch was selected for the current study because it combines the advantages of a biodegradable design, is not prone to encapsulation risks of nondegradable patches (12,13), exhibits appropriate mechanical features, and incorporates bioinductive effects from ECM. The isolated effect from ECM independent of the mechanical effect was not considered, as previous studies demonstrated that intact ECM patches did not increase cardiac stiffness (12). Finally, the lack of cellular components in this approach offers a simple and reproducible way to enhance heart remodeling without the challenges associated with cellular therapy in clinical translation.

CHRONIC MODEL. In the current study, we sought to verify how this biohybrid polymer-ECM patch features could benefit hearts with longstanding MI. The question of the optimal time for a biomaterial-based intervention to positively impact post-infarct LV remodeling has been considered in other settings. Yoshizumi et al. (14) verified that although rats in which ventricular wall hydrogel injection at different time points post-MI all presented improvement versus infarcted controls, the best LV echocardiographic results were obtained when injections were applied 3 days after MI. Although this and similar studies suggest there is a window for optimal benefit (15), the question of how beneficial an intervention might be at much later time points has not been addressed. Most cardiac patch implant studies, including those with cell delivery, were performed within a short period after MI induction (16,17). In this model, we intended to mimic a relevant clinical situation, that is, when patients begin treatment long

FIGURE 7 Histologic Assessment of LV With MT Staining at Base, Mid LV, and Apex

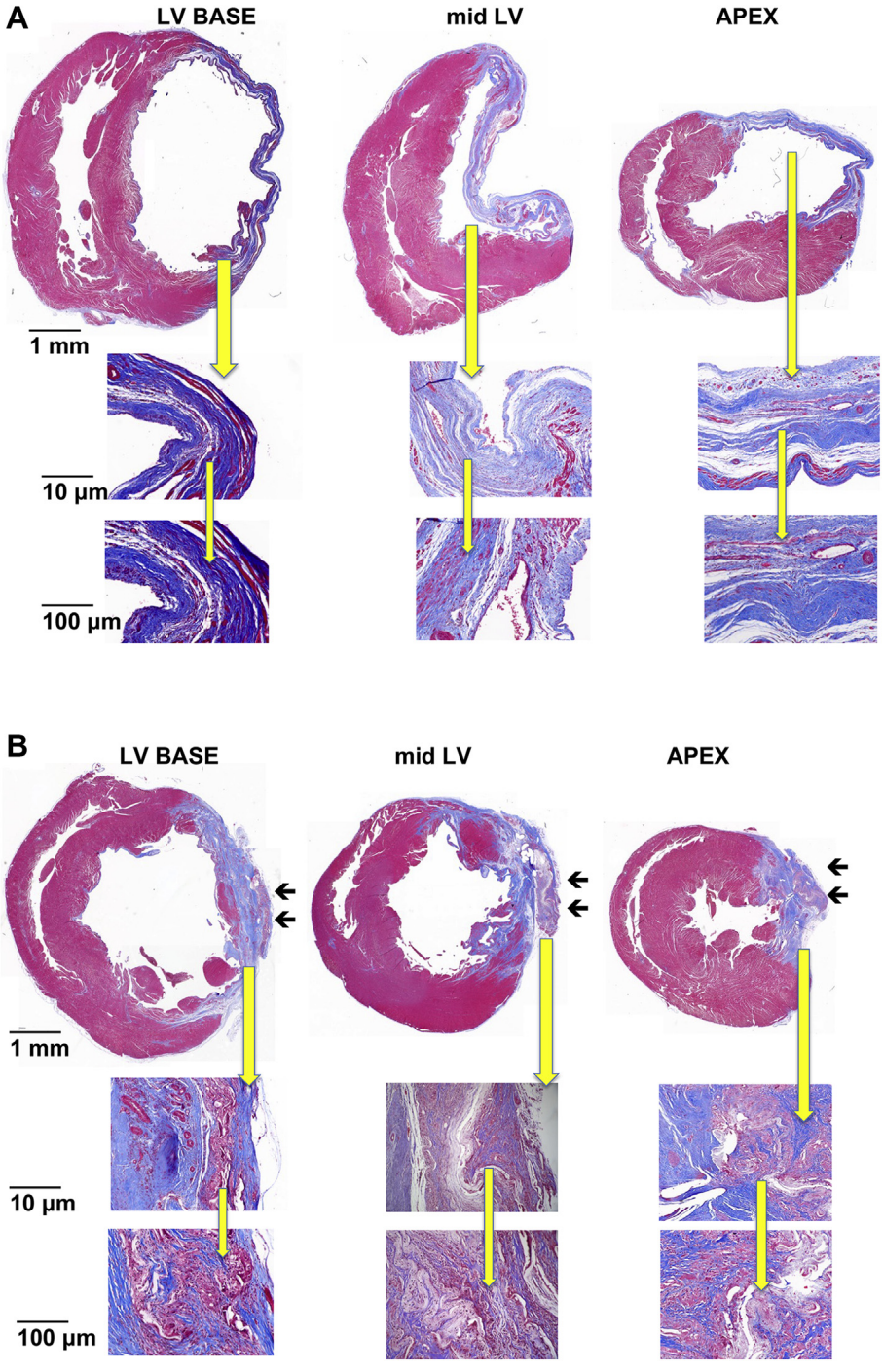

(A) MT staining of control group heart (infarcted, nonpatched) showing healthy tissue **(red)** and a large infarcted segment **(blue)** that is very narrow in width. At higher magnifications, the infarcted area is seen as a region rich in collagen but with low cellularity. This pattern is observed at all 3 levels. **(B)** MT staining of patch group heart showing healthy tissue **(red)** and an infarcted segment **(blue)** with a remnant of the remodeled patch **(black arrows)**. At higher magnifications, cell infiltration is seen around the patch, near the scar area. This pattern is verified at all 3 levels. LV = left ventricle; MT = Masson trichrome.

FIGURE 8 Macroscopic Assessment of Hearts

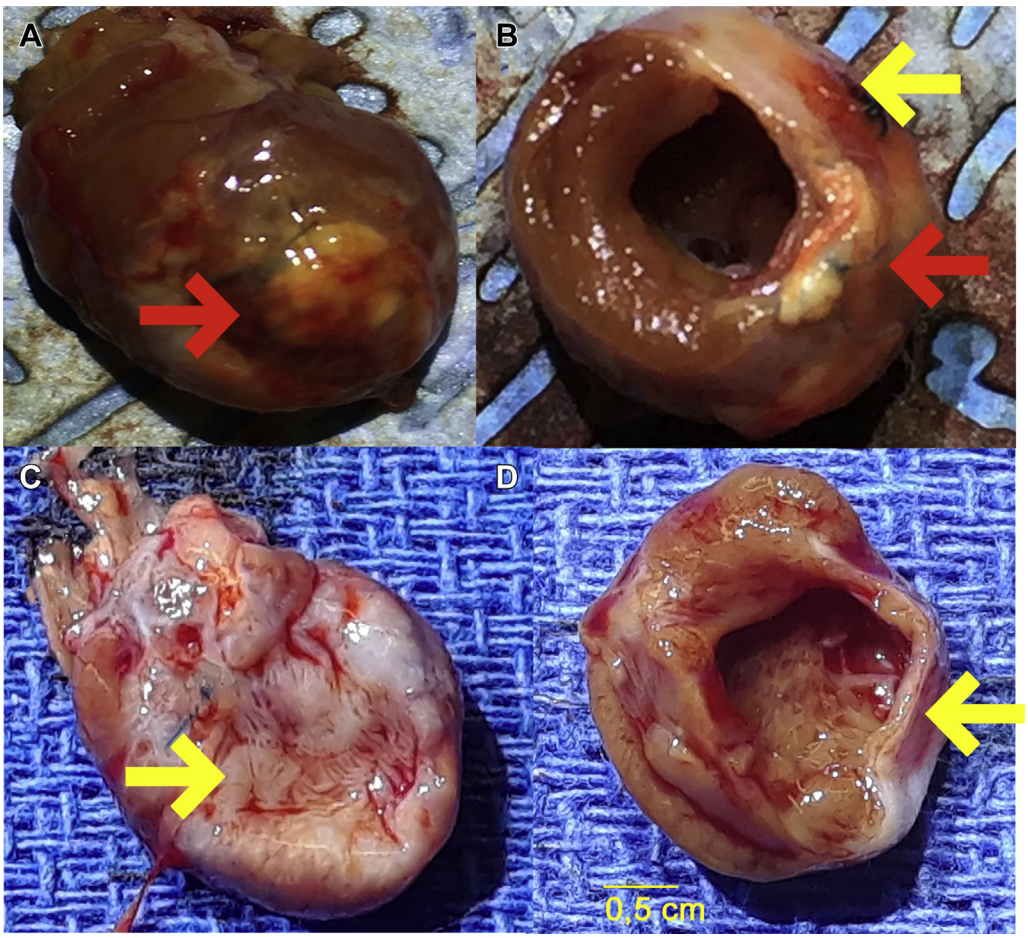

(A) Patched heart showing patch applied over infarcted area **(red arrow)**. **(B)** Transverse section of patch heart and its relation to infarcted area (**yellow arrow**; patch indicated by **red arrow**). **(C)** Control heart with wide dyskinetic area **(yellow arrow)**. **(D)** Transverse section of control heart with large infarcted area that is very narrow in width **(yellow arrow)**.

after MI. Because much of the remodeling in terms of myocardial tissue loss, thinning, and scar formation has already occurred and functional parameters have deteriorated substantially, whether this negative trend could be arrested or potentially reversed is of interest. This is particularly true when the applied patch was not delivering cells or when operating under the hypothesis that new functional tissue would result from the intervention. Our results showing functional preservation or improvement support the concept that the patch and the tissue that replaces it result in an LV having altered mechanical properties and morphology that are of benefit, despite the advanced stage of disease.

In our model, relevant large infarcts had developed, and the average initial EF at pre-treatment among the 3 groups was 33.1 ± 8.5%. We considered this initial EF value as a strength of this model, emphasizing its ability to induce severe heart dysfunction at the time of treatment. The morphological echocardiographic data showed evidence of dilated cardiomyopathy progression from baseline pre-treatment to 8 weeks post-treatment only in nonpatched groups (Figure 5). The higher levels of EF and %FS in the patched versus both nonpatched groups 4 and 8 weeks after treatment were consistent with reports of ECM patch applied 4 weeks after MI (18). In that report, the verified pre-treatment EF was around 60%, much higher than for this study. In the current work, for the subgroup with very low initial EF, %FS increased from 13.0 ± 2.8% to 18.5 ± 5.3% ($p = 0.002$), and EF increased from 26.8 ± 5.3% to 36.8

FIGURE 9 LV Thickness and Percent Infarct Size Among Groups

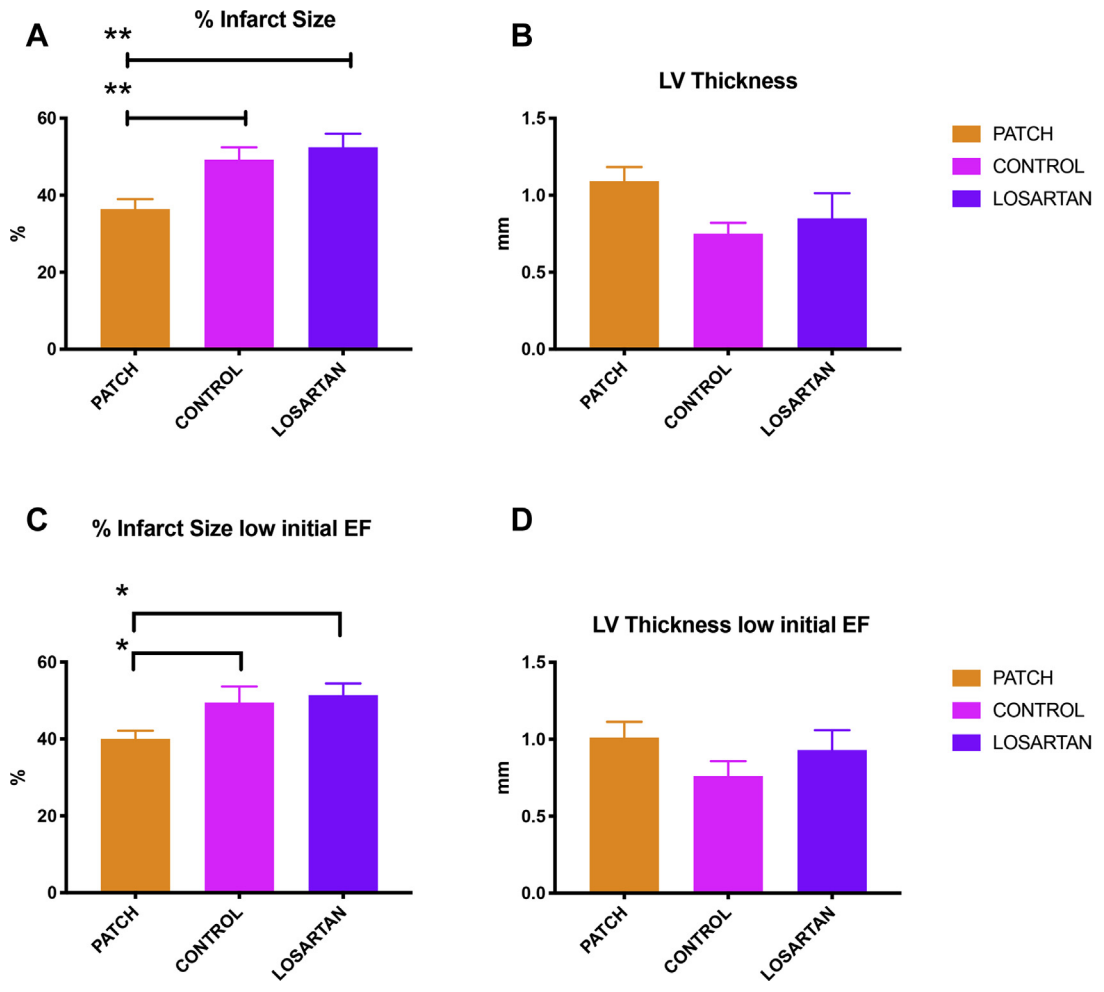

(A) Percent infarct size related to healthy tissue was lower in patch-treated animals than in control and losartan animals. **(B)** LV thickness was not significantly different among groups. **(C, D)** In animals with initial very low EF (<35%), percent infarct size was lower in patch-treated animals than in both nonpatched animals **(C)**, whereas LV thickness did not show differences **(D)**. Data are expressed as mean ± SEM. *$p < 0.05$; **$p < 0.01$. Abbreviations as in Figure 3.

± 9.5% ($p = 0.002$) from pre-treatment to 8 weeks post-treatment with patch (Figure 6). Although not quantitatively analyzed, we observed higher sphericity in control and losartan group animals, whereas patched hearts resembled more closely the healthy LV geometry. This finding is consistent with remodeling improvement.

The smaller infarct size was verified in patched animals. Similar results were reported previously with polymeric patches (3) and with the same PECUU-ECM patch applied 2 weeks post-MI (5). Our current study indicates that even with advanced remodeling and inconsistent covering of the infarcted region, the patch implant was able to alter the remodeling phenomenon, possibly by limiting infarct expansion, resulting in a proportionally lower infarcted area related to healthy tissue. In previous studies, different biodegradable patches were related to improvement in LV thickness, and this effect of minimizing wall thinning was generally associated with echocardiographic improvements (3,5,9).

The inclusion of a group of rats assigned to receive the AT_1R losartan was designed to compare the patch effect to a pharmaceutical intervention aimed at addressing a similar scenario. Losartan was selected because it is a Class 1, Level of Evidence: B drug for

FIGURE 10 Ex Vivo LV Pressure-Volume Testing

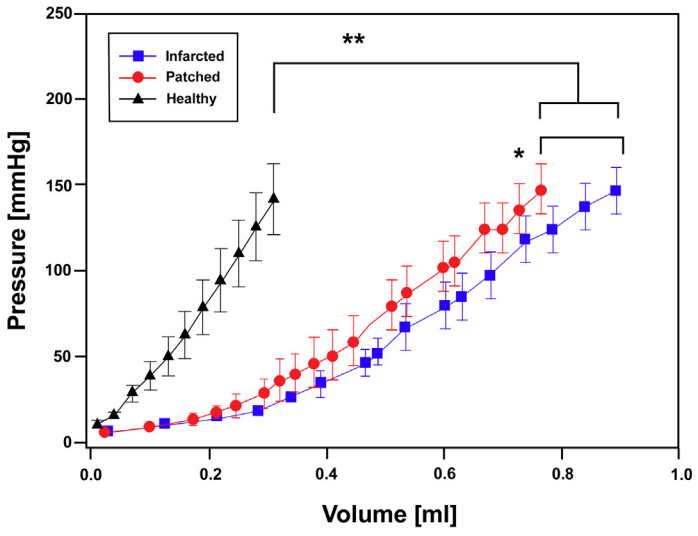

The 2 infarcted groups (patched and control) were much more compliant than the healthy group; however, the patched hearts showed greater stiffening than did the infarcted controls (n = 15). Data are expressed as mean ± SEM. *p < 0.01; **p < 0.001.

post-MI patients and is widely used clinically, especially for patients with large LV infarcts (8). Oral administration of losartan in a sucrose solution or sugar paste, similar to the protocol utilized here, has been used in several studies that showed equivalent bioavailability to other methods highly effective for chronic oral administration in laboratory rodents (19,20). Experimental evidence in animal models has shown that losartan, when given for 8 weeks before ischemia, protected hearts from the effects of nandrolone in an ischemia-reperfusion Langendorff model (21). Oral administration of losartan was associated with reductions of MI size when rats received the drug for 4 or 10 weeks pre-ischemia (22) or when swine received the drug as an acute intravenous infusion (23). In our model, losartan was started 5 days after MI induction, mimicking a situation in which the drug is administered only after MI. Most of the previous models were ischemia-reperfusion acute studies, with Langendorff evaluations (21-24) or much shorter follow-up after infarct (25).

The lack of difference in the echocardiographic and infarct size endpoints between losartan and control may be explained by the competitive risk of death effect bias, in which the echocardiographic and infarct size endpoints could only be verified in the surviving animals at the end of protocol. Given that more control animals died than losartan animals, there may have been a selection in which only the healthiest control animals remained alive. Regardless of this effect, the improvements observed with patch in this study were significantly better than the administration of a class 1 drug frequently utilized for clinical treatment of post-MI patients.

PECUU-ECM PATCH EFFECTS. Earlier reports have shown improvement with biomaterial-based therapy in cardiac remodeling, even without delivery of cells (4,26,27). Peptides and other subcellular components derived from the processed ECM are hypothesized to be the agents of ECM bioactivity that induce angiogenesis and constructive remodeling potential (28). The biohybrid PECUU-ECM patch was intended to combine the mechanical properties of PECUU with the bioactive features of ECM gel. The PECUU-ECM patch, when implanted in a post-MI rat model (5), elicited higher M2 expression and neovascularization than polymer patches alone. Sarig et al. (18) verified a time-dependent M2/M1 ratio increase after ECM patch implant 30 days after MI, but the M2/M1 ratio and the vascular density with the ECM patch were not different from the values in untreated controls 30 days after implant. Comparing our results to previous studies (5,18), as we measured immunofluorescence only 16 weeks post-MI, the effects on vascularization and M2 did not show a clear effect of the ECM-bearing patch on either parameter. This may be attributed to the different substrate (more advanced infarct) to which the patch was applied and the late assessment time, as these results were similar to those verified by Sarig et al. (18) 30 days after MI.

Patch implants have been shown to improve the stiffness of the ventricular wall, and this mechanical effect may trigger more positive remodeling and benefits in LV function. Mechanistically, preventing chamber dilation and mitigating LV wall thinning reduce wall stress and, according to Laplace's law, have been the rationale for implanting epicardial restraint devices (5,12). Surgical ventricular restoration surgeries also rely on mechanical effects promoted by decrease of LV diameter and indirect exclusion of the thinned scarred tissue, augmenting actual LV thickness and triggering remodeling improvements (29). Mechanistically, our results suggest the immunomodulatory effects related to polymer and ECM patches may be present but are not sustained in the long term, while the mechanical compliance tests indicate greater stiffening over patch-treated infarcted hearts at the same time. This finding suggests that the sustained benefits with the PECUU-ECM patch, at least in the long term, may be related to the patch's ability to induce mechanical alterations

on the combined underlying LV and the former patch area that has been infiltrated with tissue. Although not sustained, the early biological effects may set up the longer-term mechanical benefit.

The importance of patch mechanics and degradation time for patches applied onto chronic infarcts such as those used in this study remains unaddressed. Earlier reports on patches applied 2 weeks post-MI suggest that slower degrading polymers may be more beneficial than faster degrading polymers (13), and that a stiff, nondegradable expanded polytetrafluoroethylene patch had a detrimental effect of cardiac function (3). Nondegradable patches have been used clinically as restraint devices (30,31). The CorCap device (Acorn Cardiovascular Inc., St Paul, Minnesota), a polyester mesh applied around the ventricles to provide complete circumferential diastolic support, resulted in reductions of LV end-diastolic volumes and improvement by at least 1 level in New York Heart Association functional class compared to clinical treatment, but it has not prevented evolution to end-stage HF (30). Other encircling cardiac restraint devices presented similar results (31). This approach was accompanied by the risk of encapsulating the heart in a combined nondegradable polymer and fibrous capsule that would present challenges to further interventions (30,31). The idea of implanting a degradable biohybrid patch, with a biologically active ECM gel and a mechanically supportive scaffold, in order to enhance LV remodeling and function is markedly different from the idea of simply restraining the myocardium to block further dilation.

TRANSLATIONAL CHALLENGES. The results of the current study reinforce the question whether delivery of precursor cells or humoral factors is critical for LV remodeling improvement (32). In clinical studies, biodegradable epicardial patches have been applied as a medium to carry and deliver cells and factors (33). Recent experimental studies have emphasized the benefits of patches made of ECM seeded with synthetic cardiac stromal cells or hydrogel-based patches with extracellular vesicles secreted from cardiomyocytes derived from induced pluripotent stem cells on EF recovery and infarct size (34,35). The improvements verified by these studies are in agreement with our results and emphasize the potential of implanting devices not requiring direct cellular therapy.

Regulatory challenges to manufacture and clinically translate use of complex devices raise the question of costs versus benefits, even if a benefit over simpler approaches can be demonstrated. Related to this issue is the structural question as to whether regeneration or improved remodeling is the more realistic goal. Several studies have reached toward the ambitious objective of generating contracting cardiomyocytes using highly complex patch devices (1,2,4). Along these lines, recent reports have integrated cardiac cells, scaffolds, nanocomposites, and electroactive polymers to synchronize contractility and provide controlled drug release (1,36). Despite the desirable features of such approaches, the pathway to clinical translation clearly is challenging. The greater simplicity of biomaterial implantation without cellular components, even though the biomaterial in this study is of greater complexity than, for example, an expanded polytetrafluoroethylene patch, may offer remodeling benefit without seeking to regenerate new functional myocardium and may find applicability even in chronic scenarios as studied in this report.

Clinical delivery of injectable biomaterials to infarcted LV by intravenous, transcoronary, or transendocardial means has been applied experimentally and in a few clinical protocols (37,38). These approaches have shown feasibility but irregular results, as they are associated with limitations of the efficiency of material delivery and material retention in heart tissue. Epicardial patches can be easily implanted over ischemic or scarred tissue during open cardiac procedures such as coronary artery bypass grafting or LV assist device implantation (33). However, there is a large number of HF patients with advanced functional class (generally advanced age and especially frail), thus requiring more hospitalizations and higher costs. These patients are not likely candidates for heart transplantation or LV assist devices. Minimally invasive surgical procedures to implant the patch without performing full sternotomy could result in significant improvement in these patients. This might be accomplished with thoracoscopic or subxiphoid procedures, with the patch implanted over epicardium with or without sutures (e.g., with adhesives). Furthermore, even though all animal models investigated were based on ischemia models, this form of treatment may be worthy of evaluation in nonischemic HF patients because it is based on remodeling features present in both ischemic and nonischemic patients.

STUDY LIMITATIONS. This study is a rodent model, so the scale of effects from patch size to tissue ingrowth response will vary in larger models. Because chronic MI mostly occurs in older patients, it could be beneficial to test whether the same method used in older animals would also show positive patch effects.

Large animal studies, with models that mimic advanced HF, should be attempted to evaluate how this treatment would apply to humans in the chronic stage. Losartan usually is taken with spironolactone, beta-blockers, platelet antiaggregants, and statins. In clinical reality, patients taking this combination of drugs may have better remodeling than the remodeling attempted in this protocol. The possibility of administering this full combination of drugs was considered too complex for this study. The concept of applying this material-based, cell-free patch over an infarcted region was not intended to specifically address arrhythmia related to infarcted tissue, and no arrhythmias were noted. However, the problem with introducing or facilitating arrhythmia can be a concern in the context of cellular therapy (4,32), and further specific studies would be required to better assess this risk. As the echocardiographic measurements were recorded based on area measurements rather than direct volumetric measurements, this methodology may have misestimated the effects of the patch on LV structure and function. Finally, the standardized 6-mm circumference patch frequently was not able to cover the entire infarcted area at the advanced stage. Use of a larger patch possibly would induce better mechanical support and improvement.

CONCLUSIONS

The biohybrid PECUU-ECM patch applied over a chronic LV infarct resulted in less LV dilation better EF and %FS compared to nontreated control and losartan-treated groups. The remodeling benefit was particularly notable in a subgroup of the sickest rats with very low initial EF in which the echocardiographic endpoints were found to improve after treatment. Patch-treated animals presented a smaller infarct size and stiffer LV than animals that were not patched. These results indicate that this biohybrid PECUU-ECM patch was able to improve cardiac function in the post-infarction remodeling process even after extensive remodeling and high cardiac function impairment had occurred. This technological approach may hold promise for future translation to use in patients in a chronic scenario.

ACKNOWLEDGMENTS The authors acknowledge the Badylak lab for use of the microscope and the McGowan Institute for Regenerative Medicine small animal facility personnel, HongBin Jiang and Yasumoto Matsumura, for consultations on conducting the experiments.

FUNDING SUPPORT AND AUTHOR DISCLOSURES

This work was funded by the Commonwealth of Pennsylvania, the RiMED Foundation, and the Italian Ministry of Education and Research (MIUR DOT1720429). Dr. Silveira-Filho was personally funded by FAPESP (São Paulo State Funding agency). The authors have reported that they have no relationships relevant to the contents of this paper to disclose.

ADDRESS FOR CORRESPONDENCE: Dr. William R. Wagner, McGowan Institute for Regenerative Medicine, University of Pittsburgh, Bridgeside Point II, 450 Technology Drive, Suite 300, Pittsburgh, Pennsylvania 15219, USA. E-mail: lindembergms@icloud.com.

PERSPECTIVES

COMPETENCY IN MEDICAL KNOWLEDGE: The study results showing the potential for application of a simple patch, even after advanced LV remodeling has occurred, may offer an attractive option for promoting better LV remodeling in a wide variety of patients. Patients with advanced HF who are not suitable for more aggressive treatments but who frequently are candidates for procedures such as resynchronization therapy might benefit from minimally invasive epicardial patch implant to interrupt HF evolution.

TRANSLATIONAL OUTLOOK: In order to achieve clinical translation, this approach should be attempted in larger animals (e.g., swine) using models that mimic advanced HF. Minimally invasive patch implant delivery methods with straightforward application should be developed in these models.

REFERENCES

1. Feiner R, Engel L, Fleischer S, et al. Engineered hybrid cardiac patches with multifunctional electronics for on line monitoring and regulation of tissue function. Nat Mater 2016;15:679–85.

2. Lancaster JJ, Sanchez P, Repetti GG, et al. Human induced pluripotent stem cell-derived cardiomyocyte patch in rats with heart failure. Ann Thorac Surg 2019;108:116977.

3. Fujimoto KL, Tobita K, Guan J, et al. Placement of an elastic biodegradable cardiac patch on a subacute infarcted heart leads to cellularization with early developmental cardiomyocyte characteristics. J Card Fail 2012;18:585–95.

4. Rane AA, Chrisman KL. Biomaterials for treatment of myocardial infarction. A 5-year update. J Am Coll Cardiol 2011;58:2615–29.

5. D'Amore A, Yoshizumi T, Luketich SK, et al. Bi-layered polyurethane-extracellular matrix cardiac patch improves ischemic ventricular wall remodeling in a rat model. Biomaterials 2016;107:1–14.

6. Reis LA, Chiu LLY, Feric N, Fu L, Radisic M. Biomaterials in myocardial tissue engineering. J Tissue Eng Regen Med 2016;10:11–28.

7. Moorthi A, Tyan YC, Chung TW. Surface-modified polymers for cardiac tissue engineering. Biomater Sci 2017;5:1976–87.

8. O'Gara PT, Kushner FG, Ascheim DD, et al. 2013 ACCF/AHA guideline for the management of ST-elevation myocardial infarction: a report of the American College of Cardiology Foundation/American Heart Association Task Force on Practice Guidelines. J Am Coll Cardiol 2013;61:e78–140.

9. Hashizume R, Fujimoto KL, Hong Y, et al. Biodegradable elastic patch plasty ameliorates left ventricular adverse remodeling after ischemia-reperfusion injury: a preclinical study of a porous polyurethane material in a porcine model. J Thorac Cardiovasc Surg 2013;146:391–9.

10. D'Amore A, Stella JA, Wagner WR, Sacks MS. Characterization of the complete fiber network topology of planar fibrous tissues and scaffolds. Biomaterials 2010;31:5345–54.

11. Faulk DM, Johnson SA, Zhang L, Badylak SF. Role of the extracellular matrix in whole organ engineering. J Cell Physiol 2014;229:984–9.

12. Mewhort HEM, Svystonyuk DA, Turnbull JD, et al. Bioactive extracellular matrix scaffold promotes adaptive cardiac remodeling and repair. J Am Coll Cardiol Basic Trans Science 2017;2:450–64.

13. Hashizume R, Hong Y, Takanari K, Fujimoto KL, Tobita K, Wagner WR. The effect of polymer degradation time on functional outcomes of temporary elastic patch support in ischemic cardiomyopathy. Biomaterials 2013;34:7353–63.

14. Yoshizumi T, Zhu Y, Jiang H, et al. Timing effect of intramyocardial hydrogel injection for positively impacting left ventricular remodeling after myocardial infarction. Biomaterials 2016;83:182–93.

15. Kadner K, Dobner S, Franz T, et al. The beneficial effects of deferred delivery on the efficiency of hydrogel therapy post myocardial infarction. Biomaterials 2012;33:2060–6.

16. Wei H, Chen C, Lee W, et al. Bioengineered cardiac patch constructed from multilayered mesenchymal stem cells for myocardial repair. Biomaterials 2008;29:3547–56.

17. Piao H, Kwon J, Piao S, et al. Effects of cardiac patches engineered with bone marrow-derived mononuclear cells and PGCL scaffolds in a rat myocardial infarction model. Biomaterials 2007;28:641–9.

18. Sarig U, Sarig H, de-Berardinis E, et al. Natural myocardial ECM patch drives cardiac progenitor based restoration even after scarring. Acta Biomater 2016;44:209–20.

19. Diogo LN, Faustino IV, Afonso RA, Pereira SA, Monteiro EC, Santos AI. Voluntary oral administration of losartan in rats. J Am Assoc Lab Anim Sci 2015;54:549–56.

20. McLachlan J, Beattie E, Murphy MP, et al. Combined therapeutic benefit of mitochondria-targeted antioxidant, MitoQ10, and angiotensin receptor blocker, losartan, on cardiovascular function. J Hypertens 2014;32:555–64.

21. Marques-Neto SR, Ferraz EB, Rodrigues DC, et al. AT1 and aldosterone receptors blockade prevents the chronic effect of nandrolone on the exercise-induced cardioprotection in perfused rat heart subjected to ischemia and reperfusion. Cardiovasc Drugs Ther 2014;28:125–35.

22. Safari F, Hajizadeh S, Shekarforoush S, Bayat G, Foadoddini M, Khoshbaten A. Influence of ramiprilat and losartan on ischemia reperfusion injury in rat hearts. J Renin Angiotensin Aldosterone Syst 2011;13:29–35.

23. Parlakpinar H, Ozer MK, Acet A. Effects of captopril and angiotensin II receptor blockers (AT1, AT2) on myocardial ischemia-reperfusion induced infarct size. Cytokine 2011;56:688–94.

24. Abbasloo E, Najafipour H, Vakili A. Chronic treatment with apelin, losartan and their combination reduces myocardial infarct size and improves cardiac mechanical function. Clin Exp Pharmacol Physiol 2020;47:393–402.

25. Kiss K, Fekete V, Pálóczi J, et al. Renin-angiotensin-aldosterone signaling inhibitors losartan, enalapril, and cardosten prevent infarction induced heart failure development in rats. Altern Ther Health Med 2016;22:10–7.

26. Rao SV, Zeymer U, Douglas PS, et al. Bioabsorbable intracoronary matrix for prevention of ventricular remodeling after myocardial infarction. J Am Coll Cardiol 2016;68:715–23.

27. Nelson DM, Ma Z, Fujimoto KL, Hashizume R, Wagner WR. Intramyocardial biomaterial injection therapy in the treatment of heart failure: Materials, outcomes and challenges. Acta Biomater 2011;7:1–15.

28. Wassenaar JW, Gaetani R, Garcia JJ, et al. Evidence for mechanisms underlying the functional benefits of a myocardial matrix hydrogel for post-MI treatment. J Am Coll Cardiol 2016;67:1074–86.

29. Dor V. Left ventricular reconstruction for ischemic cardiomyopathy. J Card Surg 2002;17:180–7.

30. Mann DL, Kubo SH, Sabbah HN, et al. Beneficial effects of the CorCap cardiac support device: 5 year results from the Acorn Trial. J Thorac Cardiovasc Surg 2012;143:1036–42.

31. Naveed M, Mohammad IS, Xue L, et al. The promising future of ventricular restraint therapy for the management of end-stage heart failure. Biomed Pharmacother 2018;19:25–32.

32. Menasché P. The future of stem cells: should we keep the "stem" and skip the "cells"? J Thorac Cardiovasc Surg 2016;152:345–9.

33. Menasché P, Vanneaux V, Hagège A, et al. Human embryonic stem cell-derived cardiac progenitors for severe heart failure treatment: first clinical case report. Eur Heart J 2015;36:2011–7.

34. Huang K, Ozpinar EW, Su T. An off-the-shelf artificial cardiac patch improves cardiac repair after myocardial infarction in rats and pigs. Sci Transl Med 2020;12:eaat9683.

35. Liu B, Lee BW, Nakanishi K. Cardiac recovery via extended cell-free delivery of extracellular vesicles secreted by cardiomyocytes derived from induced pluripotent stem cells. Nat Biomed Eng 2018;2:293–303.

36. Noor N, Shapira A, Edri R, Gal I, Wertheim L, Dvir T. 3D Printing of personalized thick and perfusable cardiac patches and hearts. Adv Sci 2019;6:1900344.

37. Traverse JH, Henry TD, Dib N, et al. First-in-man study of a cardiac extracellular matrix hydrogel in early and late myocardial infarction patients. J Am Col Cardiol Basic Trans Science 2019;4:659–69.

38. Frey N, Linke A, Süselbeck T, et al. Intracoronary delivery of injectable bioabsorbable scaffold (IK-5001) to treat left ventricular remodeling after ST-elevation myocardial infarction: a first-in-man study. Circ Cardiovasc Interv 2014;7:806–12.

KEY WORDS biomaterial, cardiac patch, left ventricular remodeling, myocardial infarction

APPENDIX For supplemental figures and a video, please see the online version of this paper.